BJR

■ **BONE BIOLOGY**

Beta-caryophyllene prevents the defects in trabecular bone caused by Vitamin D deficiency through pathways instated by increased expression of klotho

W. Dong,
B. C. Postlethwaite,
P. A. Wheller,
D. Brand,
Y. Jiao,
W. Li,
L. K. Myers,
W. Gu

From University of Tennessee Health Science Center, Memphis, Tennessee, USA

Aims

This study investigated the effects of β-caryophyllene (BCP) on protecting bone from vitamin D deficiency in mice fed on a diet either lacking (D-) or containing (D+) vitamin D.

Methods

A total of 40 female mice were assigned to four treatment groups (n = 10/group): D+ diet with propylene glycol control, D+ diet with BCP, D-deficient diet with control, and D-deficient diet with BCP. The D+ diet is a commercial basal diet, while the D-deficient diet contains 0.47% calcium, 0.3% phosphorus, and no vitamin D. All the mice were housed in conditions without ultraviolet light. Bone properties were evaluated by X-ray micro-CT. Serum levels of klotho were measured by enzyme-linked immunosorbent assay.

Results

Under these conditions, the D-deficient diet enhanced the length of femur and tibia bones ($p < 0.050$), and increased bone volume (BV; $p < 0.010$) and trabecular bone volume fraction (BV/TV; $p < 0.010$) compared to D+ diet. With a diet containing BCP, the mice exhibited higher BV and bone mineral density (BMD; $p < 0.050$) than control group. The trabecular and cortical bone were also affected by vitamin D and BCP. In addition, inclusion of dietary BCP improved the serum concentrations of klotho ($p < 0.050$). In mice, klotho regulates the expression level of cannabinoid type 2 receptor (Cnr2) and fibroblast growth factor 23 (Fgf23) through CD300a. In humans, data suggest that klotho is connected to BMD. The expression of klotho is also associated with bone markers.

Conclusion

These data indicate that BCP enhances the serum level of klotho, leading to improved bone properties and mineralization in an experimental mouse model.

Article focus

- Cannabinoid therapy in bone loss in a vitamin D-deficient diet.
- Weight loss based on different vitamin D diets.

Key messages

- BCP improved bone properties and mineralization in an experimental mouse model.
- Mice fed a standard VD-containing diet exhibited significantly lower weight than mice receiving a VD-deficient diet.

Strengths and limitations

- This is the first reported in vivo experiment which validate BCP function in bone loss.
- Results stem from animal experiments and cannot be translated into a clinical setting.
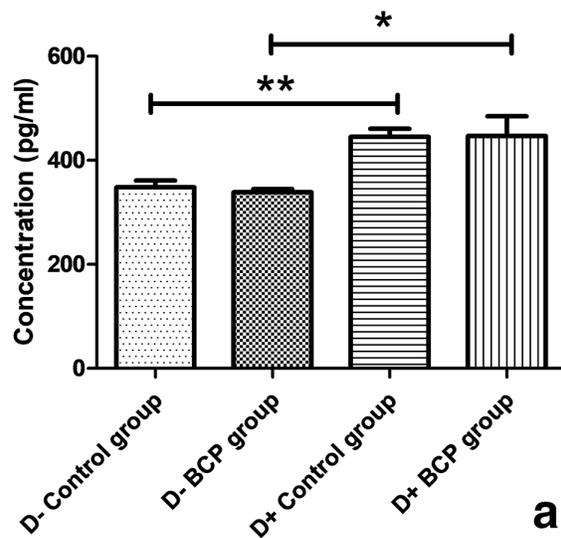
Introduction

Vitamin D is an essential element for human health that is required for normal bone mineralization and growth. Deficiency leads to vitamin D-dependent rickets in children,
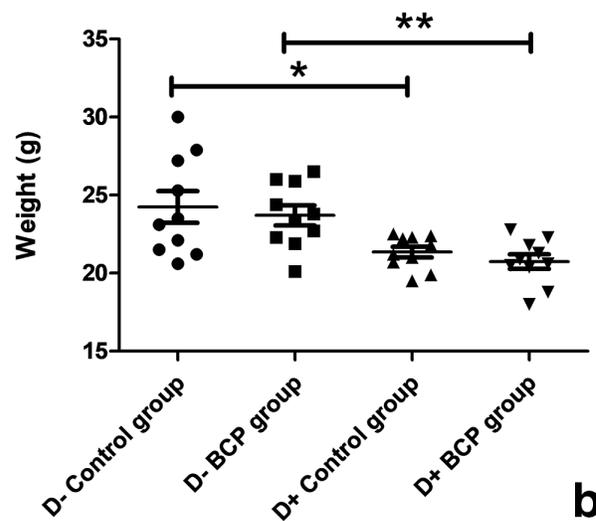
Fig. 1

Vitamin D-deficient diet led to decreased serum concentration of 25(OH)D3 in mice and increased body weight. The mice were given a diet that contained vitamin D (VD+) or lacked vitamin D (VD-) and were treated five days/week for two weeks with propylene glycol control, or with 100 μg/kg ß-caryophyllene (BCP) by oral gavage. a) Plasma 25(OH)D3 concentrations after treatment. Control groups: *p < 0.01; BCP groups: *p < 0.05. 25(OH)D3, 25-hydroxy vitamin D3, was used as a marker for vitamin D. b) Body weight after treatment. Control groups: *p < 0.05; BCP groups: *p < 0.01.

and osteomalacia and osteoporosis in adults.[1] In seeking substances to correct issues caused by vitamin D deficiency, it has become clear that existing dietary vitamin D supplements can lead to hypercalcemia.[2] Vitamin D alternatives have shown promise, but there remains a lack of evidence for their clinical usage.[3,4] Identification of other approaches, or additional therapeutic treatments to prevent bone loss and improve bone quality, is a critical next step in overcoming the side effects of current deficiency treatment strategies.

The study of endogenous cannabinoids has been focused on its effects on bone in animal models and in humans. Beta-caryophyllene (BCP) is a dietary endogenous cannabinoid that has been studied in the treatment of many diseases; it is found in plants that are ingested daily, such as clove, hemp, rosemary, and hop oil. Two receptors affect the activities of the cannabinoid, namely cannabinoid type 1 receptor (Cnr1) and cannabinoid type 2 receptor (Cnr2). BCP selectively binds to Cnr2 and functions as a full agonist for its signalling pathways.[5] Cnr2 is mainly expressed in cells of the immune system.[6] Combined deficiency of both the Cnr1 and Cnr2 receptors inhibits osteoclast development, resulting in protection against age-related bone loss.[7] In the immune system, administration of BCP regulates the expression in colon tissue of inflammation-related genes, including those that encode cytokines and chemokines, acute-phase proteins, adhesion molecules, and so forth.[8] BCP can stimulate the differentiation of bone marrow mesenchymal stem cells into osteoblasts. BCP regulates bone properties by stimulating osteoblastic mineralization, and suppressing

adipogenesis and osteoclastogenesis, in vitro.[9] It has been reported that klotho deficiency-induced arterial calcification involves a process of osteoblastic transition of smooth muscle cells and activation of bone morphogenetic protein (BMP2)-runt-related transcription factor 2 (RUNX2) signalling.[10] It has also been reported that vitamin D receptor-mediated primary induction of klotho messenger RNA (mRNA) by 1,25(OH)2D occurs in the kidneys.[11] These effects have not been studied extensively in vivo, and the role of BCP in the correction of bone properties caused by vitamin D deficiency has never been investigated.

The regulation of bone mineral density (BMD) has been linked to the enzyme klotho, but the molecular mechanisms involved are not well understood, and it is unclear whether or not BDP plays a role in this process.[12,13] Furthermore, there is no known link between BCP and klotho. Nonetheless, we hypothesized that BCP corrects the damage to bone caused by vitamin D deficiency by regulating the level of klotho in serum. The goals of this study were to investigate whether treatment with BCP improves bone properties in mice under D-deficient or D-sufficient dietary conditions, whether the level of klotho in serum increases upon treatment with BCP, and whether there is a direct connection between BCP and klotho.

Methods

Mouse treatment. Studies were conducted under animal protocols approved by the Institutional Animal Care and Use Committee (IACUC) of the University

Femur length (mm)

a

Tibia length (mm)
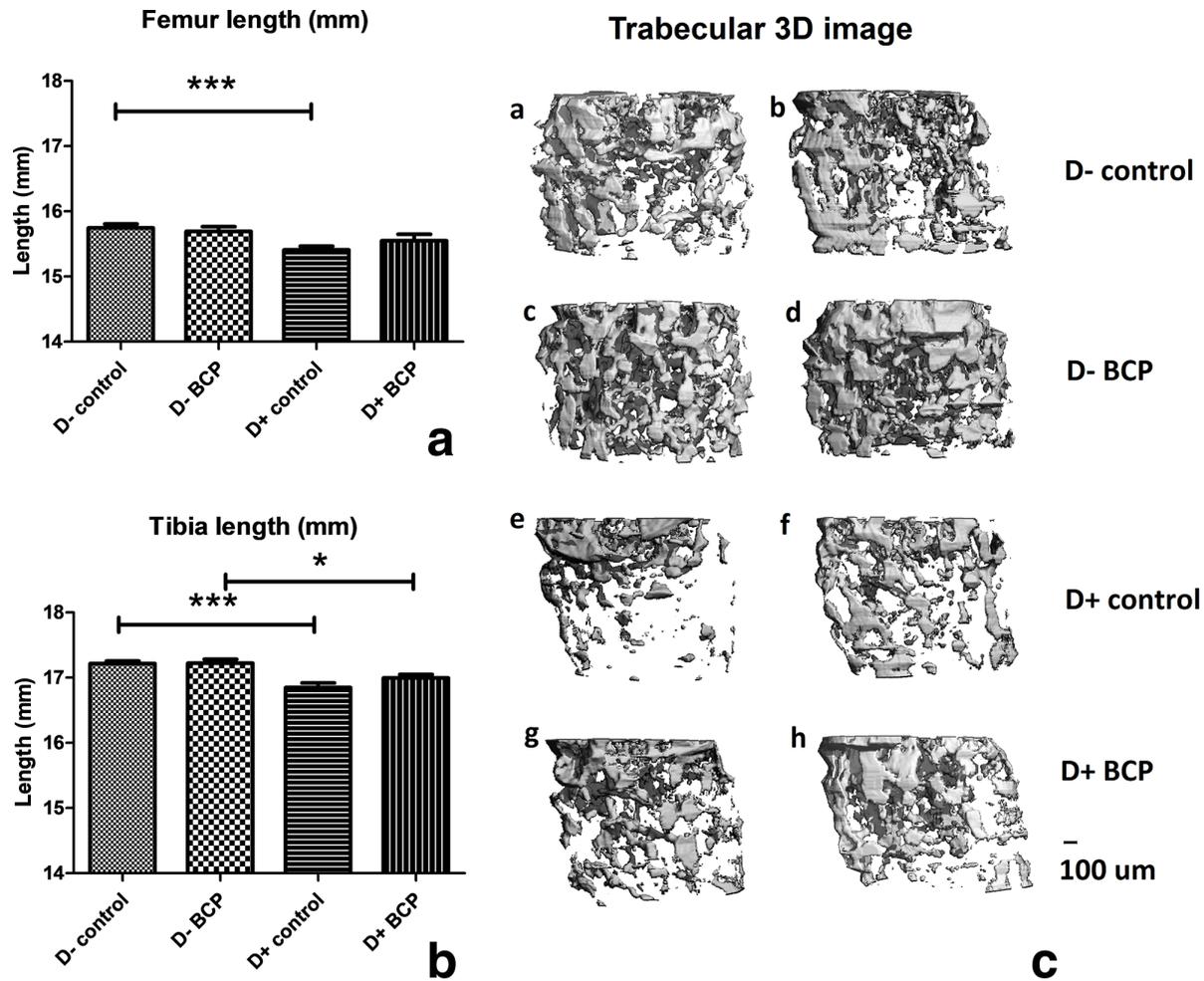

b

Trabecular 3D image

c

Fig. 2

Relative length of tibia and femur bones and 3D image reconstruction of trabecular bone in the femur. Mice were fed a vitamin D (VD)-sufficient or VD-deficient diet and received either control or ß-caryophyllene (BCP) treatment, as described in the legend to Figure 1. a) Femur length (mm). Control groups: *p < 0.001. b) Tibia length (mm). Control groups: *p < 0.001; BCP groups: *p < 0.050. a) and b) show a statistically significant shortening of tibia and femur in mice fed a vitamin D-deficient diet. c) 3D image reconstruction of trabecular bone from 100 micro-CT slices each of femur bones from the various groups of mice. Two samples are shown in each treatment group.

of Tennessee Health Science Centre at Memphis, Tennessee. Mice were housed with light-dark cycles consisting of 12 hours of light without ultraviolet (UV) light, and 12 hours of dark at an ambient temperature of 22°C (± 2°C) and a relative humidity of 30% to 60%. After weaning, 40 C57BL/6 (B6) female mice were divided into two groups (n = 20/group): 20 mice were fed with a vitamin D-deficient diet (Teklad Custom VD-deficient Diet TD.89123 (Envigo, USA), 0.47% calcium, 0.3% phosphorus), while the other 20 mice were fed with a vitamin D-containing diet (Teklad LM-485 Mouse/Rat Sterilizable Diet TD.7912 (Envigo), 1% calcium, 0.8% phosphorus). Each dietary group was divided in half, with ten mice serving as controls that were treated with propylene glycol (diluted 1:5 in intravenous (IV) saline; Sigma-Aldrich, USA) by oral gavage five days/week for two weeks, and ten mice were subjected to treatment

with 100 µg/kg BCP (Sigma-Aldrich) in IV saline by oral gavage five days/week for two weeks. Body weight was measured before treatment and after six weeks of diet treatment, just before the mice were killed.

To determine the effect of different BCP concentrations in mice fed a vitamin D-sufficient diet, we established three groups (n = 5/group) of five- to six-week-old female C57BL/6 mice and treated them with oral gavage five days/week for two weeks as follows: the control group received propylene glycol (diluted 1:5 in IV saline; Sigma-Aldrich), the 25 mg BCP group received 25 mg BCP (Elevation Terpenes, USA) in IV saline, and the 50 mg BCP group received 50 mg BCP (Elevation Terpenes) in IV saline. Body weight was measured before and after six weeks of diet treatment.

Tissue collection. Whole legs were collected and stored in 70% ethanol until they could be processed for
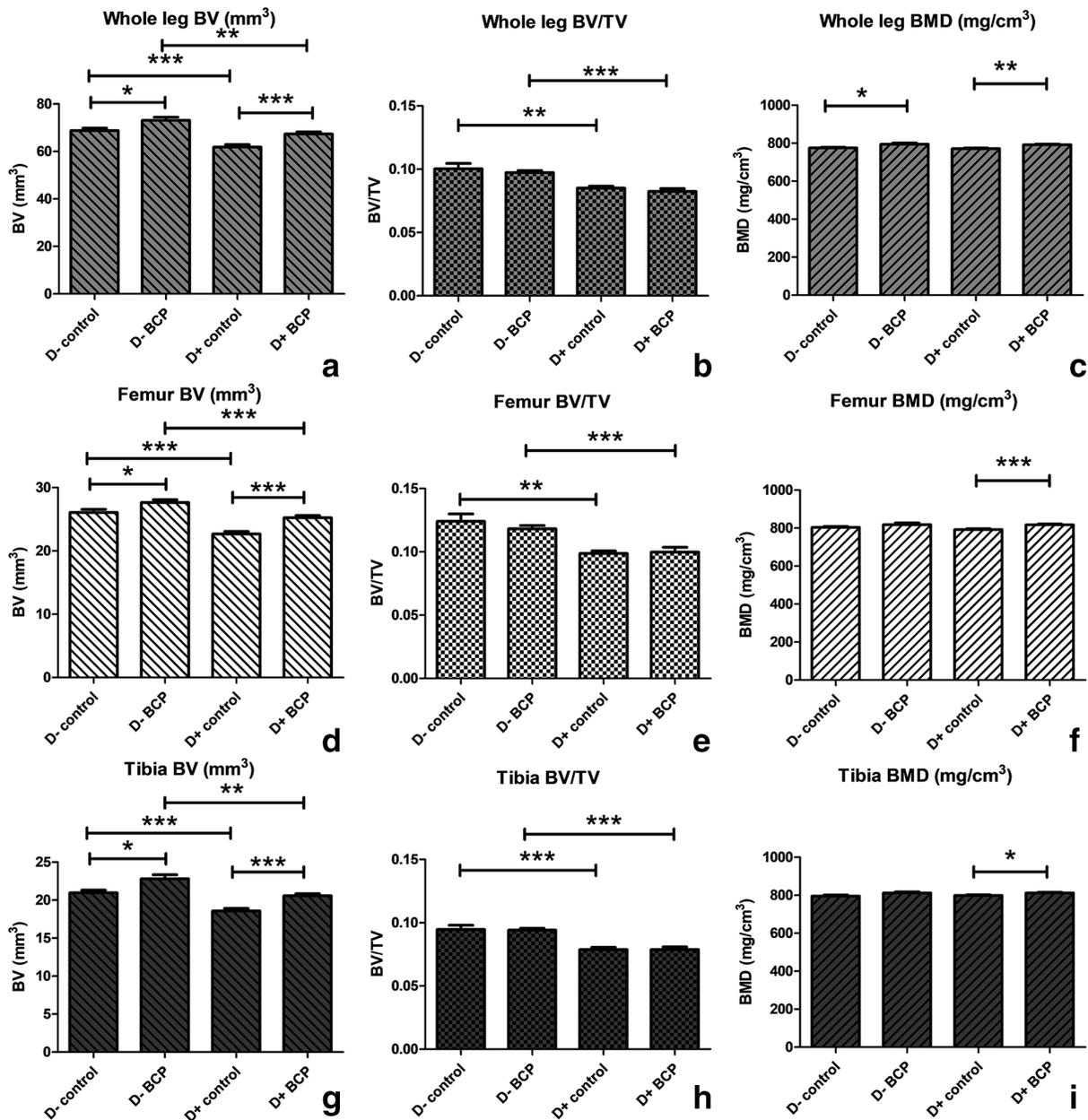
Fig. 3

Micro-CT (μCT) of whole leg, femur, and tibia reveals the properties of bone in the presence or absence of vitamin D in mice treated with ß-caryophyllene (BCP). Mice were fed a vitamin D-sufficient or -deficient diet and received control or BCP treatment, as described in the legend to Figure 1. Bone samples from the whole leg, femur, and tibia of mice from each treatment group were subjected to μCT using a μCT 40 desktop μCT scanner (Scanco Medical, USA). a), b), and c) reflect the results of scans of whole leg; d), e), and f) show scans of femur; and g), h), and i) show scans of tibia. Bone volume (BV) is depicted in panels a), d), and g); bone volume/total volume (BV/TV) is shown in panels b), e), and h); bone mineral density (BMD) is depicted in panels c), f), and i). *p < 0.050; **p < 0.01; ***p < 0.001.

high-resolution micro-CT (μCT). Whole blood was also collected at the time the mice were killed; this was processed as described below.

Micro-CT analysis. To quantitatively assess the structural changes associated with genetic variation, morphometric and architectural indices were determined from microtomographic examinations. In this study, μCT

was used to scan the whole leg, tibia, and femur, and to characterize the overall and regional bone profiles. All measurements and analysis were performed using the software included with the SCANCO μCT40 instrument. The bone samples were placed in an 8 mm diameter sample holder in 70% ethanol and immobilized with plastic foam. A μCT 40 desktop scanner (Scanco

Table I. Analysis of trabecular bone properties in the femur of mice fed vitamin D-sufficient or vitamin D-deficient diet, and treated with ß-caryophyllene or mock-treated (control).

Property	Group				p-values			
	D- control	D- BCP	D+ control	D+ BCP	D- control vs D- BCP	D+ control vs D+ BCP	D- control vs D+ control	D- BCP vs D+ BCP
Mean VOX-TV, mm³ (SD)	1.42 (0.08)	1.44 (0.08)	1.29 (0.04)	1.32 (0.10)	0.632	0.395	0.000	0.007
Mean VOX-BV, mm³ (SD)	0.13 (0.05)	0.19 (0.09)	0.05 (0.01)	0.09 (0.03)	0.054	0.002	0.001	0.004
Mean VOX-BV/TV, % (SD)	0.09 (0.03)	0.13 (0.06)	0.04 (0.01)	0.06 (0.02)	0.050	0.001	0.001	0.004
Mean Conn-Dens., mm² (SD)	26.96 (16.30)	51.86 (34.29)	9.03 (5.29)	18.92 (10.49)	0.059	0.019	0.007	0.015
Mean TRI-SMI (SD)	3.08 (0.29)	2.76 (0.43)	3.32 (0.19)	3.05 (0.20)	0.067	0.006	0.047	0.079
Mean DT-Tb.N, 1 / mm (SD)	3.59 (0.47)	4.07 (0.71)	2.76 (0.36)	3.13 (0.29)	0.095	0.022	0.000	0.002
Mean DT-Tb.Th, μm (SD)	0.06 (0.01)	0.07 (0.00)	0.05 (0.00)	0.06 (0.01)	0.216	0.001	0.000	0.012
Mean DT-Tb.Sp, μm (SD)	0.28 (0.03)	0.25 (0.04)	0.37 (0.06)	0.32 (0.03)	0.071	0.042	0.001	0.000
Mean apparent density, g/cm³ (SD)	114.78 (23.45)	145.24 (32.69)	76.00 (10.62)	98.08 (12.62)	0.029	0.001	0.000	0.001
Mean material density, g/cm³ (SD)	528.62 (23.67)	531.77 (25.80)	499.67 (30.15)	518.23 (17.37)	0.779	0.113	0.029	0.188
Mean TRI-TV, mm³ (SD)	1.41 (0.08)	1.42 (0.08)	1.27 (0.04)	1.30 (0.10)	0.631	0.399	0.000	0.007
Mean TRI-BV, mm³ (SD)	0.12 (0.05)	0.19 (0.09)	0.04 (0.01)	0.08 (0.03)	0.055	0.002	0.001	0.004
Mean TRI-BV/TV (SD)	0.09 (0.03)	0.13 (0.06)	0.03 (0.01)	0.06 (0.02)	0.050	0.001	0.001	0.004
Mean TRI-BS, mm² (SD)	5.72 (1.67)	8.15 (2.94)	2.64 (0.62)	4.18 (1.20)	0.039	0.003	0.000	0.002
Mean TRI-BS/BV (SD)	48.87 (5.32)	45.45 (4.78)	60.75 (5.99)	51.57 (5.35)	0.148	0.002	0.000	0.015
Mean TRI-Tb.N, 1 / mm (SD)	2.03 (0.57)	2.84 (0.94)	1.04 (0.25)	1.59 (0.38)	0.034	0.002	0.000	0.002
Mean TRI-Tb.Th, μm (SD)	0.04 (0.00)	0.04 (0.00)	0.03 (0.00)	0.04 (0.00)	0.160	0.002	0.000	0.015
Mean TRI-Tb.Sp, μm (SD)	0.49 (0.15)	0.34 (0.11)	0.98 (0.24)	0.62 (0.14)	0.020	0.001	0.000	0.000
Mean TRI-DA (SD)	1.46 (0.07)	1.49 (0.05)	1.48 (0.17)	1.46 (0.11)	0.190	0.870	0.737	0.494

BMD, bone mineral density; BS, bone surface; BV, bone volume; BV/TV, trabecular bone volume; Conn-Dens, connectivity density; DA, degree of anisotropy; DT, distance transformation; SD, standard deviation; SMI, structure model index; (Tb.N), trabecular number; (Tb.Sp), trabecular separation; (Tb.Th), trabecular thickness; TRI, triangularization of surface; VOX, voxels.

Medical, USA) was used to scan the samples at 11.5 μm resolution, at an energy level of 55 keV, with 2,000 projections, an integration time of 300 ms, and an intensity of 145 μA. Morphometric and architectural parameters of bones were assessed, and realistic 3D visual models were constructed for each bone sample by selecting the volumes of interest (VOIs). 3D trabecular parameters were evaluated using a fixed Gaussian filter, and a threshold of 220 for the cancellous bone and 260 for the cortical envelope.

No rotation was used (0.0°). Bone volume (BV), bone volume/total volume (BV/TV), and BMD were measured in the bones of the whole leg, femur, and tibia. Morphometric indices were calculated on two bone types in the femur, namely cortical bone in the diaphysis and trabecular bone in the metaphysis. In order to standardize the measurements for each sample, the centre of the knee joint was determined by visualizing slices and moving upward until the tops of the tibial condyles disappeared altogether. This was considered the midline of the knee joint. Measurements were standardized by counting the number of uniform slices either above or below the midline, depending on the specific analysis. For the femoral trabecular bone, we selected 100 slices above the midline to determine total volume (TV), BV, BV/TV, connectivity density (Conn-Dens), structure model index (SMI), number of trabecular bones (Tb.N), thickness of trabecular bones (Tb.Th), separation degree of trabecular bones (Tb.Sp), apparent BMD, and material BMD. For the cortical bone, we selected the same 100 slices to analyze TV, BV, BV/TV, cortical porosity (Ct. Porosity), cortical thickness (Ct.Th), SMI, apparent BMD, and material BMD. The lengths of the femur and tibia were also measured. The tibia was measured from
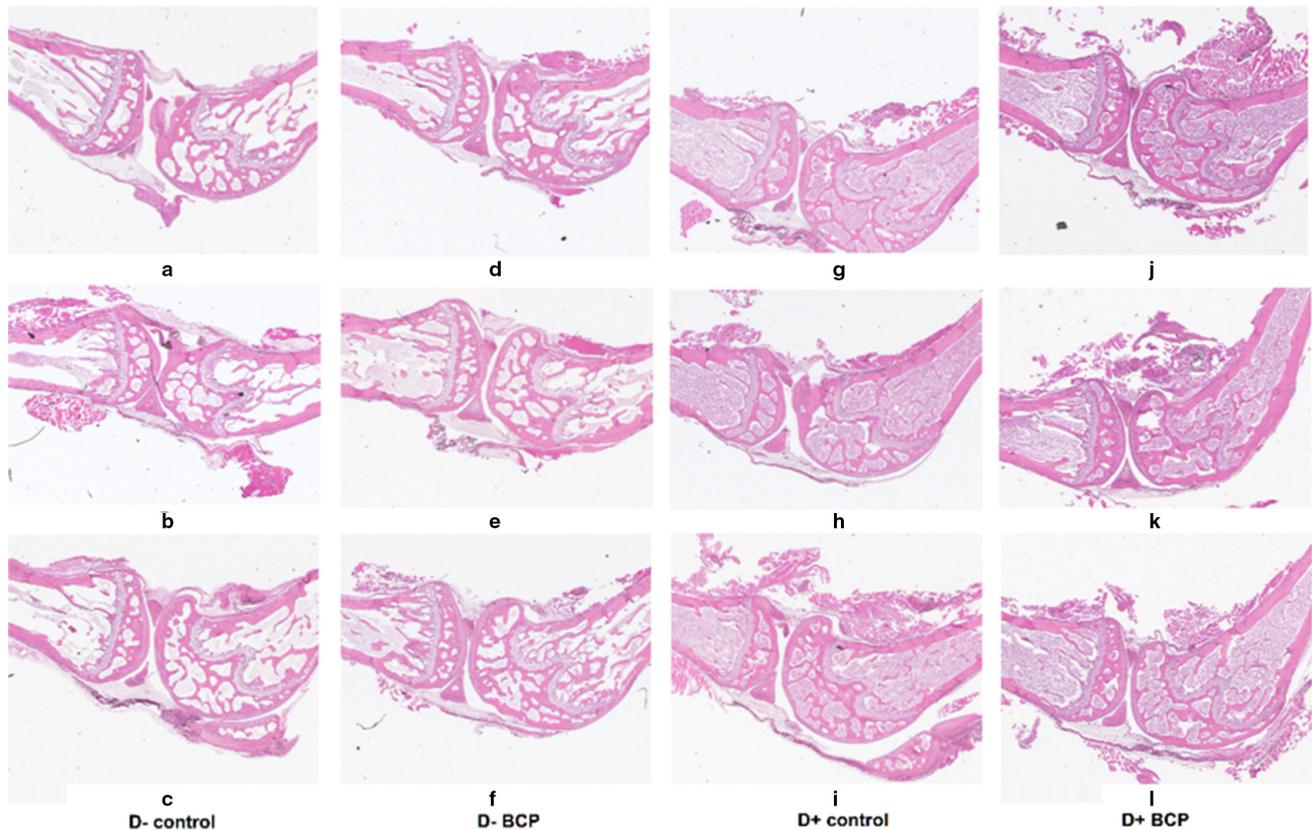
Fig. 4

Histopathological features of knee joint tissues in mice from different groups at the endpoint of the experiment. a) to c) Vitamin D-deficient diet (D-) control group. d) to f) D- ß-caryophyllene (BCP) group. g) to i) Standard vitamin D-sufficient diet (D+) control group. j) to l) D+ BCP group.

the top of the tibial condyle to the most distal tibial bone slice, and the femur was measured from the base of the femoral head to the most distal femoral condyle.

Histological analysis. Histological analysis was performed at the Dr. Silva Laboratory at the Washington University School of Medicine in St. Louis, Missouri. The process for haematoxylin and eosin (H&E) staining is briefly described below. After µCT analysis, the bone tissues were cut and underwent decalcification, dehydration, and paraffin embedding. Then, the bone tissues were cut with a thickness of 5 µm using the tissue slicer. The slices were stained with the H&E staining solution.

Blood treatment and ELISA analysis. Blood samples collected from the mice were centrifuged at 4°C for ten minutes, serum supernatants were collected, and serum samples were stored at -80°C until laboratory analysis. Sera were collected from five mice in each treatment group and pooled. Serum levels of 25-hydroxyVD3 (25(OH)D3), BCP, and klotho were evaluated using an enzyme-linked immunosorbent assay (ELISA). Klotho was measured in three replicates from pooled sera from each treatment group using a mouse ELISA Kit from MyBioSource (USA), following the manufacturer's instructions. According to the protocol, the Mouse kit used a two-site sandwich ELISA to measure klotho amount with the antibody which had been pre-coated onto the microplate. First, controls

and samples were added into the wells where the klotho binds to the immobilized antibody. Second, any solution with unbound substances was removed. Next, a biotin-conjugated antibody specific for klotho was added to the wells. After washing, streptavidin-conjugated horseradish peroxidase (HRP) was added to the wells. Following another wash, a substrate solution was added to the wells to let colour develop in proportion to the amount of klotho bound in the initial step. Finally, the colour development was stopped, and the colour intensity was measured.

Statistical analysis. All statistical analyses were performed using GraphPad Prism 5 (GraphPad, USA). Comparisons between groups when data were normally distributed were made with the two-tailed independent-samples t-test. A p-value less than 0.05 was considered to be significant, and is labelled with single asterisks (*), $p < 0.01$ was labelled with two asterisks (**) to denote higher significance, and $p < 0.001$ was labelled with three asterisks (***) to denote highest significance.

Results

The effect of vitamin D on loss of body weight. We used an experimental animal model to examine the effects of dietary vitamin D and BCP treatment on body weight and bone growth. Female mice were assigned to one of four
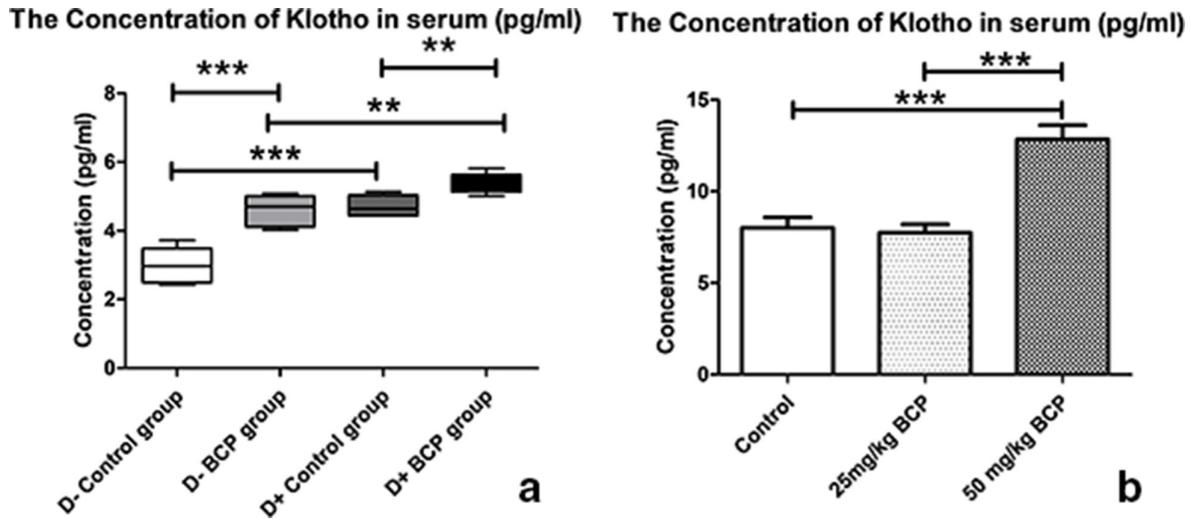
Fig. 5

Detection of klotho in the serum of mice fed on vitamin D-containing and vitamin D-deficient diets that were treated with ß-caryophyllene (BCP) or with propylene glycol control. Whole blood was collected from mice, the serum fraction was isolated by centrifugation, sera from individuals in each group were pooled, and the relative levels of klotho were detected by enzyme-linked immunosorbent assay (ELISA). a) The effect of vitamin D and BCP treatment on serum levels of klotho. b) The effect of different concentrations of BCP treatment on levels of klotho in serum. Three groups of mice (n = 5/group) were fed on a vitamin D-sufficient diet for six weeks. For the last two weeks, they were treated by oral gavage for five days/week with propylene glycol control or with 25 mg/kg or 50 mg/kg BCP. Serum samples from each group were pooled and tested for the presence of klotho by ELISA. **p < 0.010; ***p < 0.001.

treatment groups (n = 10/group): vitamin D+ diet with propylene glycol control, vitamin D+ diet with BCP, vitamin D-deficient diet with propylene glycol control, and vitamin D-deficient diet with BCP. The mice were fed with the appropriate diet for six weeks and housed in the absence of UV light. We began by determining the serum levels of 25-hydroxy vitamin D3 (25(OH)D3) in mice from each group. As shown in Figure 1a, the serum of mice with dietary vitamin D sufficiency (the vitamin D+ with control and vitamin D+ with BCP groups) contained a significantly higher concentration of 25(OH)D3 than the mice that were fed a vitamin D-deficient diet (D-deficient with control or D-deficient with BCP), regardless of the absence (control groups; p < 0.01) or presence of BCP (p < 0.05). This result validated our assumption that, in the absence of UV light, feeding the mice for six weeks on a vitamin D-deficient diet led to their anticipated deficiency.

Sufficiency of vitamin D can lead to weight loss. In one study, vitamin D levels were inversely correlated with BMI (r = -0.22, p = 0.025), suggesting some potential benefits for individuals living with obesity, although this remains to be investigated in a prospective study.[14] For individuals living with obesity, an eight-week low-calorie diet programme supplemented with vitamin D led to a significant decrease in inflammatory markers, compared with the same diet with a placebo supplement.[15] Obesity is associated with low plasma levels of 25-hydroxy-vitamin D, which can result from vitamin D deficiency.[16–19] Therefore, we compared body weights of the mice from each group before and after treatment. Mice fed on standard vitamin D-containing diet exhibited significantly lower weight than mice receiving a vitamin D-deficient diet,

regardless of whether they were treated with BCP (p < 0.010) or with propylene glycol control (p < 0.050), as shown in Figure 1b.

Effects of vitamin D and BCP on length of femur and tibia bones. To determine the effect of vitamin D and BCP on bone growth, we measured the length of femur and tibia bones in mice after the six-week D-sufficient or D-deficient diet in the control and BCP-treated groups. The mice on the D-deficient diet (D-) exhibited femur and tibia lengths that were significantly longer than those of mice fed normal vitamin D-containing diet (D+), as shown in Figures 2a and 2b (p < 0.001). Interestingly, BCP treatment resulted in no change in femur length (Figure 2a) and only a small, statistically significant change in tibia length using two-tailed independent-samples *t*-test (Figure 2b).

Effects of BCP and vitamin D on bone volume, trabecular bone volume, and bone mineral density. We used high-resolution µCT to further analyze the bones of the vitamin D-fed and vitamin D-deficient mice in the absence or presence of BCP treatment. We determined the bone volume (BV), trabecular bone volume – which is depicted as the ratio of BV to total volume (BV/TV) – and bone mineral density (BMD) of the whole leg, femur, and tibia (Figure 3). The mice on a vitamin D-deficient diet exhibited a statistically significant increase in BV (p < 0.010) and BV/TV ratio (p < 0.010) of whole leg (Figures 3a and 3b), femur (Figures 3d and 3e), and tibia (Figures 3g and 3h), relative to mice fed a normal vitamin D-sufficient diet (D+ groups). The presence or absence of vitamin D in the diet did not significantly affect BMD (Figures 3c, 3f and 3i). Interestingly, mice fed either a vitamin D-sufficient or
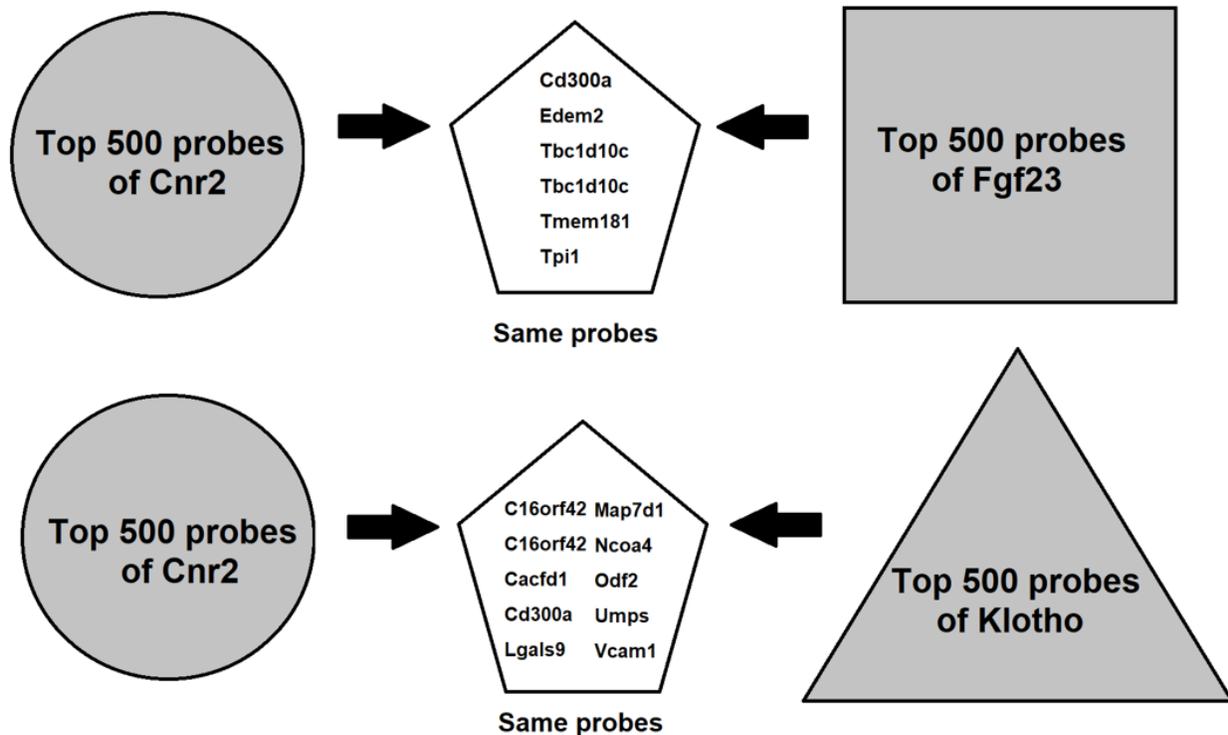
Fig. 6

Comparisons between cannabinoid type 2 receptor (Cnr2), fibroblast growth factor 23 (Fgf23), and klotho in top 500 probes.

vitamin D-deficient diet and treated with 100 µg/kg BCP exhibited higher BV (Figures 3a, 3d and 3g) and BMD (Figures 3c, 3f and 3i), which was statistically significant compared to those observed for propylene glycol-treated controls ($p < 0.050$).

Effects of BCP and vitamin D on trabecular bone of femur. Trabecular bone is found at the ends of long bones, such as the femur, and in the spinal column. It is composed of sparse rods and plates of bone (trabeculae) that comprise 20% of trabecular bone volume and are interspersed by bone marrow. Trabecular bone provides strength and elasticity. It is less dense and relatively more fragile than the cortical or compact bone that comprises the dense outer bone surface. Cortical bone is strong, rigid, and provides strength for weight-bearing.[20] Loss of either trabecular or cortical bone mass, for example due to age, menopause, or osteoporosis, leads to decreased strength and stability and increased risk of fracture.[21–24] The microarchitecture of trabecular bone is particularly important, since loss of bone mass can lead to decreased structural connectivity.[24]

The decrease in bone volume (BV/TV) we observed in Figure 3 led us to examine the microarchitecture of trabecular bone using our µCT data. We performed a 3D image reconstruction using 100 slices of trabecular bone from the femur, as shown in Figure 2c. Strikingly, we observed a higher degree of connectivity in trabecular bone from mice fed a vitamin D-deficient diet (D- groups)

than that observed in mice fed a standard vitamin D-sufficient diet (D+ groups). The trabecular bone from mice treated with BCP appeared to be denser than that from propylene glycol-treated control animals, suggesting that bone loss may have been lessened by the treatment, or that it resulted in the repair of trabecular bone.

The 3D reconstructed images led us to further investigate the microarchitecture of femoral trabecular bone. Several parameters were used to evaluate the spatial morphological structure of femoral trabecular bone, including trabecular thickness (Tb.Th), trabecular number (Tb.N), and trabecular separation (Tb.Sp). In the D+ groups, Tb.N and Tb.Th values decreased, whereas the Tb.Sp values increased relative to those observed in the D- groups. These data indicate that bone catabolism in the presence of vitamin D is greater than bone anabolism, suggesting that osteoporosis occurred in the mice fed the vitamin D-sufficient diet. The structure model index (SMI) allows quantification of bone structure in terms of the number of rods and plates comprising the structure determined by µCT.[25] A structure such as trabecular bone composed of rods and plates will have a value between 0 (all plates) and 3 (all rods). As such, the SMI will increase during osteoporosis as the bone becomes more porous. As shown in Table I, the SMI and Tb.Sp values were higher for the D+ groups than those of the D- groups, consistent with increased porosity. Treatment of the D+ group with BCP resulted in statistically
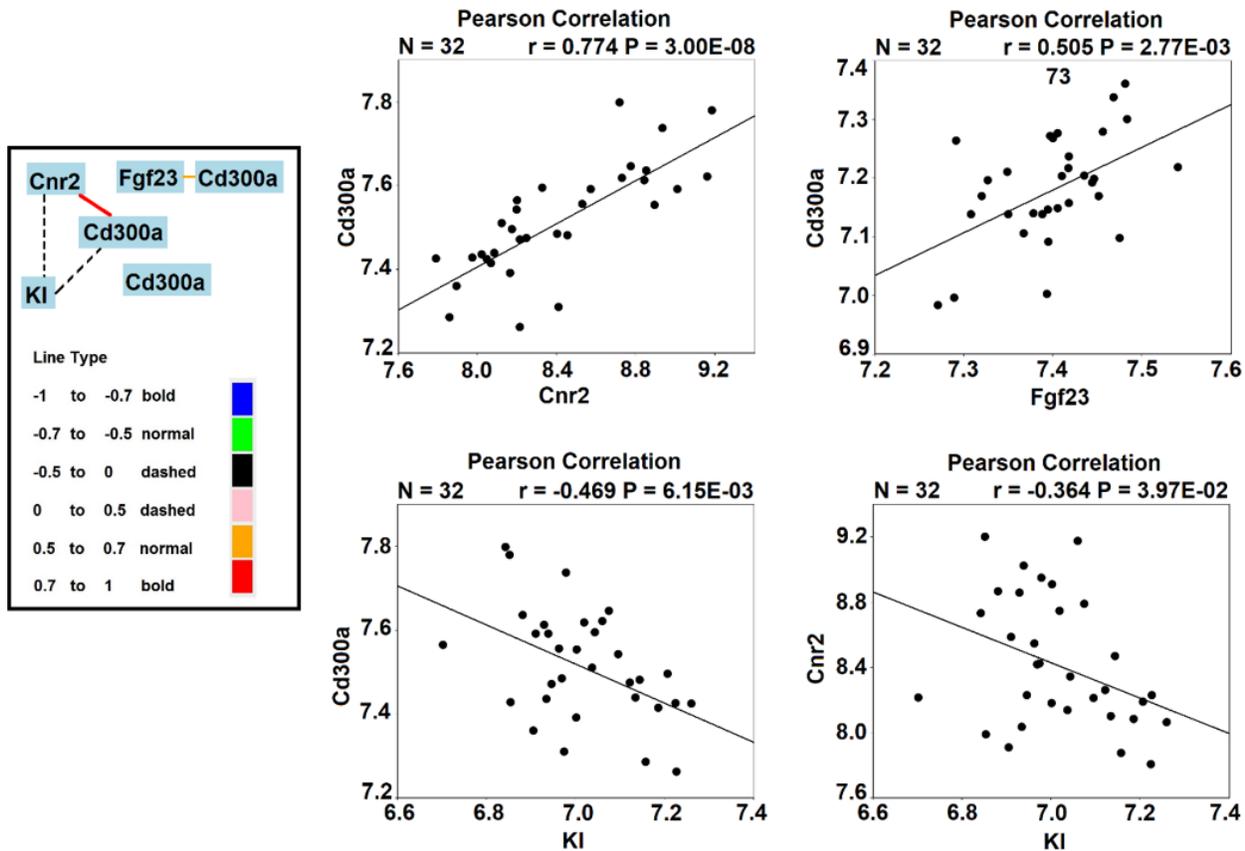
Fig. 7

Correlations between fibroblast growth factor 23 (Fgf23), klotho, cannabinoid type 2 receptor (Cnr2), and CD300a in mice.

significant increases (p = 0.022, p = 0.001) in Tb.N and Tb.Th, and decreases (p = 0.042, p = 0.006) in Tb.Sp and SMI compared to the D+ control group. However, in D- mice, treatment with BCP was less effective and led to statistically significant changes in only Tb.N (decrease, p = 0.034) and Tb.Sp (increase, p = 0.020) relative to the control group (D- control).

Effects of BCP and vitamin D on cortical bone from the femur. We repeated the analysis using slices of cortical bone from the femora of mice from the four groups. The effect of the vitamin D-deficient diet and BCP treatment on cortical bone was less pronounced than that seen for trabecular bone. There was a slight effect on bone thickness that was not seen for all groups (Supplementary Table i). In mice fed on a D+ diet, cortical bone was thicker for the BCP-treated group than the control group (p = 0.038). Interestingly, the cortical bone of femora from the D- control group was thicker than that of the D+ control group (p = 0.002).

Histological comparison. After μCT analysis, the whole hindlimb was used in the H&E staining. Compared with D- diet groups, D+ diet groups showed greater amounts of trabecular bone (Figure 4). In particular, within the two groups of D- diet, there was more trabecular bone in the femur in the BCP treatment groups than in the D- control

group, which suggests that BCP treatment prevents defects in trabecular bone.

Effects of BCP and vitamin D in klotho of serum. The enzyme klotho plays a role in the regulation of BMD.[12,13] Since our results suggest that BCP treatment may correct bone damage caused by vitamin D deficiency, we investigated whether the level of klotho in serum is altered by BCP treatment. At the end of the six-week D-sufficient or D-deficient diets in the presence and absence of BCP treatment, we collected blood from all groups and isolated the serum fractions.

We used an ELISA to measure the concentration of klotho in pooled serum samples from each group (Figure 5a). D+ control mice exhibited higher serum levels of klotho than those detected in D- control mice, which was statistically significant (p < 0.001). These data suggest that vitamin D has a positive effect on serum levels of klotho. Treatment of the mice with BCP also resulted in statistically significant increases in klotho relative to the control-treated groups for mice fed on both vitamin D-deficient (D- BCP; p < 0.001) and vitamin D-sufficient diets (D+ BCP; p < 0.010).

To verify the effect of BCP treatment on serum levels of klotho, we repeated the experiment in mice fed a vitamin D-sufficient diet and treated with varying concentrations
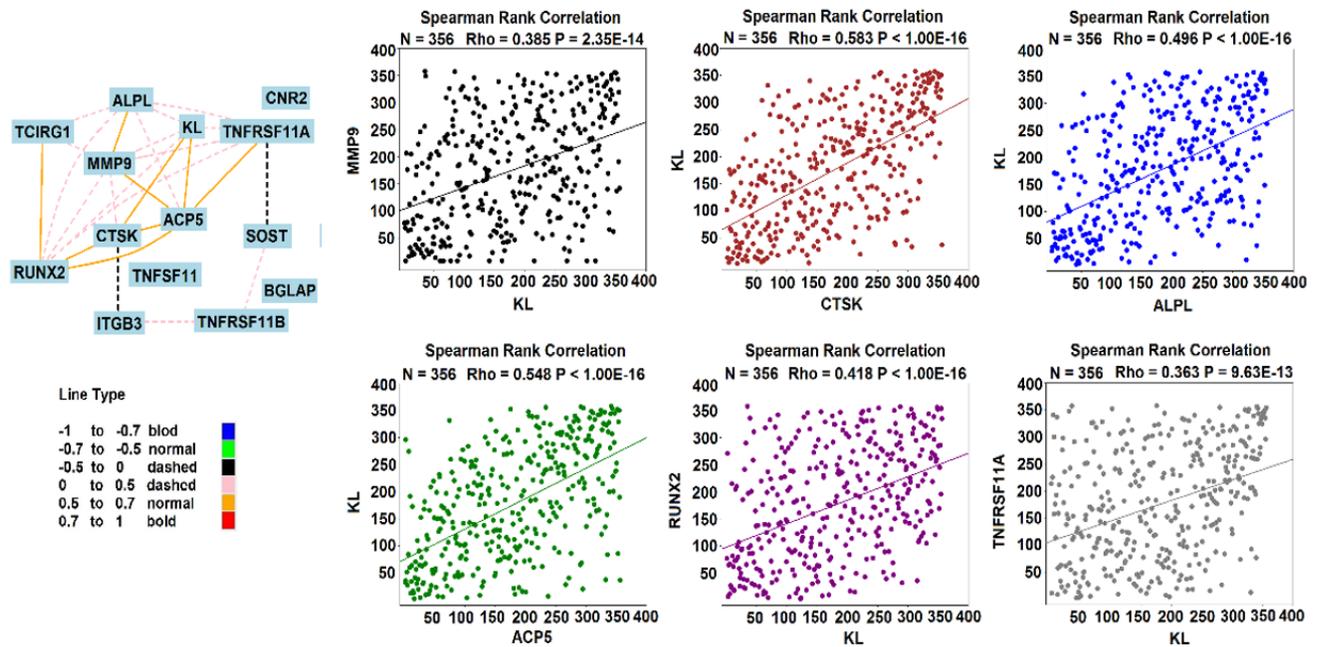
Fig. 8

Positive correlations between KL and bone markers in humans. Numbers of patients and p-values are all listed on each image. ACP5, acid phosphatase 5; ALPL, alkaline phosphatase; BGLAP, bone gamma-carboxyglutamate protein; CNR2, cannabinoid receptor 2; CTSK, cathepsin K; ITGB3, integrin subunit beta 3; KL, klotho; MMP9, matrix metallopeptidase 9; RUNX2, RUNX family transcription factor 2; SOST, sclerostin; TCIRG1, T cell immune regulator 1; TNFRSF11A, tumour necrosis factor (TNF) receptor superfamily member 11a; TNFRSF11B, TNF receptor superfamily member 11b; TNFSF11, TNF superfamily member 11.

of BCP. Three groups of mice (n = 5/group) were fed a normal diet for six weeks. For the last two weeks of the experiment, mice were treated by oral gavage five days/week with propylene glycol control or with 25 mg/kg or 50 mg/kg BCP. Whole blood was collected at the end of the experiment, and serum fractions were isolated by centrifugation, pooled by group, and analyzed for the presence of klotho by ELISA. As shown in Figure 5b, we observed a statistically significant increase in klotho detected between the control group and the 50 mg/kg BCP group (p < 0.001). These results suggest that BCP treatment can lead to the enhanced levels of klotho in serum.

Relationship between Fgf23, Kl, and Cnr2. To further investigate the mechanism of BCP on bone development, we examined the relationship between fibroblast growth factor 23 (Fgf23), klotho, and BCP (using the Cnr2 receptor for analysis), and obtained their 500 most relevant probes from GeneNetwork.[26] After comparison, we found that six probes (CD300a, Edem2, Tbc1d10c, Tbc1d10c, Tmem181, and Tpi1) are the intersection between Cnr2 and Fgf23, and ten probes (C16orf42, C16orf42, Cacfd1, CD300a, Lgals9, Map7d1, Ncoa4, Odf2, Umps, and Vcam1) are the intersection between Cnr2 and Kl (Figure 6). Among them, CD300a is the only one which could connect Cnr2, Kl, and Fgf23.

Then we compute the gene network graphic using CD300a, Cnr2, Kl, and Fgf23 (Figure 7). We chose Spring

Model layout (energy reduction) software for all graphic data depictions. The Pearson Rank coefficient was calculated separately.

It is shown in Figure 6 that CD300a has a strong positive correlation (r = 0.774) with Cnr2, and that CD300a is also positively correlated with Fgf23 (r = 0.505). Kl has negative correlations with CD300a (r = -0.469) and Cnr2 (r = -0.364).

CD300a exists on the surface of both myeloid and lymphoid cells, and the murine receptor differs from the human one in the number of ITIMs; while the human CD300a has three classic ITIMs, the murine has two. It has been reported that CD300a has a critical role in the maintenance of important cellular functions.[17,18] Previous investigators reported that the immunoreceptor CD300a controls the intensity of inflammation and dysfunction in a model of Ag-induced arthritis in mice.[17]

Verification of the relationship between KL and bone markers in humans. In order to further confirm the relationship between KL and bone development in humans, we investigated the potential gene network between KL and known bone markers (ALPL, CTSK, MMP9, ACP5, RUNX2, and TNFRSF11A) using data from tibial whole genome gene expression profiles. The data are extracted from the Genotype-Tissue Expression (GTEx) project at the GeneNetwork platform.

Our analysis revealed positive correlations between the expression level of KL and these six bone markers.

As shown in Figure 8, the positive correlations ranged from 0.363 to 0.583. Considering the large population sizes and complexity of human populations, these data support the association of the vitamin D-KL-bone loop.

Discussion

This study analyzed the effect of BCP treatment on bone morphology using a mouse model of vitamin D deficiency. A variety of bone properties were measured using µCT, and the levels of klotho protein in serum of treated mice was measured using ELISA. This is the first study of the effects of BCP on bone modifications caused by a vitamin D-deficient diet. We obtained three major interesting results from this work: the effect of BCP on bone structure and on klotho serum level, and the effect of vitamin D on loss of body weight.

Our data suggest that BCP could significantly prevent the defects in trabecular bone caused by vitamin D deficiency.[27] Our results suggest a potential application of BCP in clinical practice. Two aspects of femur trabecular structure, Tb.N and Tb.Th, were significantly higher in BCP-treated mice than those of control-treated mice, while the SMI and Tb.Sp were significantly lower in the BCP-treated mice than in control-treated mice. BMD and properties of trabecular bone are critical factors in the development of osteoporosis. BCP treatment may also improve the properties of femoral cortical bone. Currently, there are no reports on the effect of either BCP or klotho on the dynamic changes between osteoblast-osteoclast activities. However, FGF23/FGF receptor signalling has been reported to influence the osteoclast number.[28] Furthermore, a complex relationship between Fgf23, klotho, and hypoxia-inducible factor (HIF) has been detected in bone marrow.[29] Therefore, it is most likely that BCP affects the Tb.N, Tb.Th, SMI, and Tb.Sp through the klotho-anabolized Fgf23 pathway.

Our data indicate that treatment of mice with BCP increased serum levels of klotho, an effect not previously reported. These data raise two interesting issues: first, the observation that klotho levels appear to respond to BCP treatment suggests that the two are probably not acting independently of one another. Second, is BCP involved in regulating klotho levels, which then mediates bone properties? The connection between klotho and BMD has been demonstrated in a previous study.[12] For example, the expression of klotho in osteocytes controls bone formation, and has been linked to regulation of bone metabolism.[13] Serum levels of klotho have been linked to bone fracture in older adults.[12] The connection between BCP and klotho has not previously been reported. Future studies may shed light on the molecular mechanisms by which BCP may regulate klotho levels in bone.

In summary, these data suggest that BCP enhances the level of klotho in serum, thereby improving bone mineralization and bone properties of mice. In the absence of UV light, a vitamin D-deficient diet could affect multiple bone properties, including the ratio and quality of trabecular and cortical bone in mice.

Based on the results from this study and the available whole genome expression profiles of mouse femora, we constructed the first key gene which could connect BCP, Fgf23, and klotho together. Our gene network analysis showed that CD300a may play an important role in the connections between Fgf23, klotho, and BCP.[25] Our gene network revealed the potential connection between klotho and several important osteoclast marker genes, including Ctsk, Mmp9, and Acp5. Previously, klotho has not been linked to these genes. However, these genes have been discovered in the Fgf23 pathway. For example, Mmp9 and Fgf23 have been found to be coexpressed in a hypovitaminosis D kyphotic pig.[30] Our current data suggest that the BCP-klotho-Fgf23 pathway may lead to the activation of these key genes, and eventually cause the downregulation of osteoclasts, reducing either their number or their function.

Fgf23 is known as a member of the fibroblast growth factor family. It is produced by bone and acts on the kidney. Fgf23 plays a central role in mineral and bone metabolism, and also participates in phosphate and vitamin D metabolism and regulation.[31] Klotho acts as a permissive coreceptor for FGF23. FGF23 operates through a specific receptor system consisting of klotho and certain FGF receptor subtypes.[32] However, its role in the regulation of BMD has not been clearly defined. Our data suggest that BCP possibly regulates BMD and other bone properties through the FGF23-klotho pathway. It will be interesting to investigate the detailed mechanisms underlying such a regulation, and whether the effect of BCP on FGF23-klotho is indirectly through an interaction with the Ctsk, Mmp9, or Acp5.

Identification of the role of CD300a in the pathway is one important aspect for a future study. The Cd300 family modulates many immune cell processes, and this family of receptors has great potential as therapeutic targets for infectious diseases and some pathological situations. One member of the family, CD300a, is implicated in immune response signalling pathways. CD300a has also been studied as a possible biomarker.[33] However, the connection between CD300a and FGF23/Klotho has not been reported previously. It is not clear whether CD300a is the result or the trigger of the FGF23-klotho pathway. The molecular function of CD300a and its role in the FGF23/Klotho pathway remains to be determined in further studies.

In this study, we observed an increase in body weight in the vitamin D-deficient group of mice compared to the vitamin D-sufficient diet, regardless of whether BCP treatment was given. After repeating the experiment, we believe this result is reliable. This suggests that in daily life, vitamin D deficiency may lead to obesity, or that sufficient vitamin D intake may help cope with weight loss. Recently, a meta-analysis revealed an inverse association of vitamin D levels with body weight.[34] Our data agree with the report that mice fed a standard vitamin D-sufficient diet exhibited significantly lower weight than mice receiving a VD-deficient diet.

Before the application of BCP in clinical studies, the overall evaluation of its effect on human body development and biological function is essential. We only investigated the bone-relevant traits in the study; it is unknown whether any other traits are affected by BCP treatment. In particular, its long-term effect should be carefully examined.

Other important genes in the regulation of BCP-induced pathways may be missed in our analysis because our study is mainly based on the association of gene expression levels. Polymorphisms of genes have not been searched and analyzed. Thus, genes that regulate the expression levels of FGF23, klotho, and CD300a have not been explored in our study. The regulatory factors upstream of these genes await further study by expression quantitative trait locus analysis and polymorphic analysis. In the future, we should also isolate osteoclasts, osteoblasts, and osteocytes from treated mice in order to investigate precisely how some of the significantly changed parameters have developed in the mice.

Overall, our results suggest that BCP may represent a novel drug for preventing defects in trabecular bone and should be evaluated for its therapeutic benefits for osteoporosis.

Supplementary material

ê Table showing how beta-caryophyllene affects cortical bone in femur, and ARRIVE checklist.

References

1. **Holick MF**. Vitamin D: A millenium perspective. *J Cell Biochem*. 2003;88(2):296–307.
2. **Tebben PJ**, **Singh RJ**, **Kumar R**. Vitamin D-mediated hypercalcemia: mechanisms, diagnosis, and treatment. *Endocr Rev*. 2016;37(5):521–547.
3. **Lin Z**, **Marepally SR**, **Goh ESY**, **et al**. Investigation of 20S-hydroxyvitamin D$_3$ analogs and their 1α-OH derivatives as potent vitamin D receptor agonists with anti-inflammatory activities. *Sci Rep*. 2018;8(1):1478.
4. **Lin Z**, **Marepally SR**, **Ma D**, **et al**. Synthesis and biological evaluation of vitamin D3 metabolite 20S,23S-dihydroxyvitamin D3 and its 23R epimer. *J Med Chem*. 2016;59(10):5102–5108.
5. **Gertsch J**. Anti-inflammatory cannabinoids in diet: Towards a better understanding of CB(2) receptor action? *Commun Integr Biol*. 2008;1(1):26–28.
6. **Munro S**, **Thomas KL**, **Abu-Shaar M**. Molecular characterization of a peripheral receptor for cannabinoids. *Nature*. 1993;365(6441):61–65.
7. **Sophocleous A**, **Marino S**, **Kabir D**, **Ralston SH**, **Idris AI**. Combined deficiency of the Cnr1 and Cnr2 receptors protects against age-related bone loss by osteoclast inhibition. *Aging Cell*. 2017;16(5):1051–1061.
8. **Cho JY**, **Kim HY**, **Kim S-K**, **Park JHY**, **Lee HJ**, **Chun HS**. β-Caryophyllene attenuates dextran sulfate sodium-induced colitis in mice via modulation of gene expression associated mainly with colon inflammation. *Toxicol Rep*. 2015;2:1039–1045.
9. **Yamaguchi M**, **Levy RM**. β-Caryophyllene promotes osteoblastic mineralization, and suppresses osteoclastogenesis and adipogenesis in mouse bone marrow cultures *in vitro*. *Exp Ther Med*. 2016;12(6):3602–3606.
10. **Lin Y**, **Sun Z**. Klotho deficiency-induced arterial calcification involves osteoblastic transition of VSMCs and activation of BMP signaling. *J Cell Physiol*. 2022;237(1):720–729.
11. **Haussler MR**, **Livingston S**, **Sabir ZL**, **Haussler CA**, **Jurutka PW**. Vitamin D receptor mediates a myriad of biological actions dependent on its 1,25-dihydroxyvitamin D ligand: distinct regulatory themes revealed by induction of klotho and fibroblast growth factor-23. *JBMR Plus*. 2021;5(1):e10432.
12. **Chalhoub D**, **Marques E**, **Meirelles O**, **et al**. Association of serum klotho with loss of bone mineral density and fracture risk in older adults. *J Am Geriatr Soc*. 2016;64(12):e304–e308.
13. **Komaba H**, **Kaludjerovic J**, **Hu DZ**, **et al**. Klotho expression in osteocytes regulates bone metabolism and controls bone formation. *Kidney Int*. 2017;92(3):599–611.
14. **Keogh JB**, **Clifton PM**. No difference in weight loss, glucose, lipids and vitamin D of eggs for breakfast compared with cereal for breakfast during energy restriction. *Int J Environ Res Public Health*. 2020;17(23):E8827.
15. **Cheshmazar E**, **Hosseini AF**, **Yazdani B**, **Razmpoosh E**, **Zarrati M**. Effects of vitamin D supplementation on omentin-1 and spexin levels, inflammatory parameters, lipid profile, and anthropometric indices in obese and overweight adults with vitamin D deficiency under low-calorie diet: a randomized placebo controlled trial. *Evid Based Complement Alternat Med*. 2020;2020:3826237.
16. **Censani M**, **Stein EM**, **Shane E**, **et al**. Vitamin D deficiency is prevalent in morbidly obese adolescents prior to bariatric surgery. *ISRN Obes*. 2013;2013:1155.
17. **Himbert C**, **Ose J**, **Delphan M**, **Ulrich CM**. A systematic review of the interrelation between diet- and surgery-induced weight loss and vitamin D status. *Nutr Res*. 2017;38:13–26.
18. **Samuel L**, **Borrell LN**. The effect of body mass index on adequacy of serum 25-hydroxyvitamin D levels in US adults: the National Health and Nutrition Examination Survey 2001 to 2006. *Ann Epidemiol*. 2014;24(10):781–784.
19. **Stein EM**, **Strain G**, **Sinha N**, **et al**. Vitamin D insufficiency prior to bariatric surgery: risk factors and a pilot treatment study. *Clin Endocrinol (Oxf)*. 2009;71(2):176–183.
20. **Sunheimer RL**, **Graves L**. *Clinical Laboratory Chemistry*. Second ed. UK: Pearson, 2018.
21. **Legrand E**, **Chappard D**, **Pascaretti C**, **et al**. Trabecular bone microarchitecture, bone mineral density, and vertebral fractures in male osteoporosis. *J Bone Miner Res*. 2000;15(1):13–19.
22. **Ott SM**. Cortical or trabecular bone: what's the difference? *Am J Nephrol*. 2018;47(6):373–375.
23. **Thurner PJ**, **Erickson B**, **Jungmann R**, **et al**. High-speed photography of compressed human trabecular bone correlates whitening to microscopic damage. *Eng Fract Mech*. 2007;74(12):1928–1941.
24. **Brandi ML**. Microarchitecture, the key to bone quality. *Rheumatology (Oxford)*. 2009;48 Suppl 4:iv3-8.
25. **Hildebrand T**, **Rüegsegger P**. Quantification of bone microarchitecture with the structure model index. *Comput Methods Biomech Biomed Engin*. 1997;1(1):15–23.
26. **No authors listed**. Gene Network. http://www.genenetwork.org/ (date last accessed 4 July 2022).
27. **Raina DB**, **Liu Y**, **Jacobson OLP**, **Tanner KE**, **Tägil M**, **Lidgren L**. Bone mineral as a drug-seeking moiety and a waste dump. *Bone Joint Res*. 2020;9(10):709–718.
28. **Xiao L**, **Williams D**, **Hurley MM**. Inhibition of FGFR signaling partially rescues osteoarthritis in mice overexpressing high molecular weight FGF2 isoforms. *Endocrinology*. 2020;161(1):bqz016.
29. **Chow S-H**, **Chim Y-N**, **Wang J-Y**, **Wong R-Y**, **Choy V-H**, **Cheung W-H**. Inflammatory response in postmenopausal osteoporotic fracture healing. *Bone Joint Res*. 2020;9(7):368–385.
30. **Zhou Y**, **Gao Y**, **Xu C**, **Shen H**, **Tian Q**, **Deng H-W**. A novel approach for correction of crosstalk effects in pathway analysis and its application in osteoporosis research. *Sci Rep*. 2018;8(1):668.
31. **Karampela I**, **Sakelliou A**, **Vallianou N**, **Christodoulatos GS**, **Magkos F**, **Dalamaga M**. Vitamin D and obesity: current evidence and controversies. *Curr Obes Rep*. 2021;10(2):162–180.
32. **Ali E**, **Birch M**, **Hopper N**, **Rushton N**, **McCaskie AW**, **Brooks RA**. Human osteoblasts obtained from distinct periarticular sites demonstrate differences in biological function in vitro. *Bone Joint Res*. 2021;10(9):611–618.
33. **Amundson LA**, **Hernandez LL**, **Crenshaw TD**. Gene expression of matrix metalloproteinase 9 (MMP9), matrix metalloproteinase 13 (MMP13), vascular endothelial growth factor (VEGF) and fibroblast growth factor 23 (FGF23) in femur and vertebra tissues of the hypovitaminosis D kyphotic pig model. *Br J Nutr*. 2018;120(4):404–414.
34. **Dewansingh P**, **Reckman GAR**, **Mijlius CF**, **et al**. Protein, calcium, vitamin D intake and 25(OH)D status in normal weight, overweight, and obese older adults: a systematic review and meta-analysis. *Front Nutr*. 2021;8:718658.

Author information:
- W. Dong, MD, Physician, Department of Orthopaedic Surgery and Biomedical Engineering, University of Tennessee Health Science Center, Memphis, Tennessee, USA; Department of Gynecological Radiotherapy, Harbin Medical University Cancer Hospital, Harbin, China.
- B. C. Postlethwaite, MD, Rheumatologist
- P. A. Wheller, BS, Technician
- L. K. Myers, MD, General Pediatric Rheumatologist
  Department of Medicine, University of Tennessee Health Science Center, Memphis, Tennessee, USA.

- D. Brand, PhD, Professor, VA Investigator, Department of Medicine, University of Tennessee Health Science Center, Memphis, Tennessee, USA; Research Service, Veterans Affairs Medical Center, Memphis, Tennessee, USA.
- Y. Jiao, MD, MS, Associate Professor, Department of Orthopaedic Surgery and Biomedical Engineering, University of Tennessee Health Science Center, Memphis, Tennessee, USA.
- W. Li, PhD, Distinguished Professor and Director of Drug Discovery Center, Department of Pharmaceutical Sciences, University of Tennessee Health Science Center, Memphis, Tennessee, USA.
- W. Gu, PhD, Professor, Department of Orthopaedic Surgery and Biomedical Engineering, University of Tennessee Health Science Center, Memphis, Tennessee, USA; Research Service, Veterans Affairs Medical Center, Memphis, Tennessee, USA.